

THE TITANOMAGNETITE TO TITANOMAGHEMITE CONVERSION IN A WEATHERED BASALT PROFILE FROM SOUTHERN PARANÁ BASIN, BRAZIL

MARISA T. GARCIA DE OLIVEIRA^{1,*}, MILTON L. L. FORMOSO¹, MOACIR INDIO DA COSTA JR² AND ALAIN MEUNIER³

¹ Instituto de Geociências, Universidade Federal do Rio Grande do Sul, Avenida Bento Gonçalves, 9500, 91509-900 Porto Alegre, Brazil

² Instituto de Física, Universidade Federal do Rio Grande do Sul, Avenida Bento Gonçalves, 9500, 91501-970, Porto Alegre, Brazil

³ Hydrasa UMR 6532 CNRS – University of Poitiers, 40, Avenue du Recteur Pineau, 86022 Poitiers Cedex, France

Abstract—This study of magnetic minerals in a weathering profile developed on plateau basalts of the subtropical southern Paraná Basin explores the evolution of titanomagnetite to titanomaghemite. Six samples studied by optical microscopy, X-ray diffraction (XRD), electron microprobe, Mössbauer spectroscopy (MS) and scanning electron microscopy (SEM) with energy dispersive X-ray spectroscopy (EDS) support the interpretations.

The profile studied has two major parts: an upper, porous red-clay Latosol, ~2–8 m deep, separated by a stone line from an underlying alterite which has two different facies – its argillaceous alterite consists of a clayey matrix with a well-developed fissure system whereas the underlying boulder alterite consists of rock cores surrounded by highly-porous cortices of Al-goethite.

Optical microscopy showed the titanomagnetite-titanomaghemite changes in color and shape through the profile. The decrease in the lattice parameter a of the magnetic separates from the rock cores to the alterite facies was detected by XRD. Mössbauer spectroscopy identified non-stoichiometric magnetite in the rock cores and Ti-substituted maghemite in the argillaceous alterite. Chemical analysis of the titanomagnetite-titanomaghemite grains showed that the relative proportions of TiO_2 and Fe_2O_3 vary in the different weathering facies. By SEM and EDS we also detected the presence of minor components as Si, Al, Ca, K, Mg and Mn.

These results led to the interpretation that the titanomagnetites from the fresh Paraná basalts, located in the subtropical zone of Brazil, are unstable and gradually change to titanomaghemites. The evolution of these magnetic minerals is registered in the weathering facies related to climatic changes throughout geological time.

Key Words—Magnetic Minerals, Titanomaghemite, Titanomagnetite, Soils, Weathering.

INTRODUCTION

The magnetic fraction from samples of a Brazilian Latosol, which is an order of the Brazilian System of Soil Taxonomy (Camargo *et al.*, 1987; Resende *et al.*, 1995; EMBRAPA, 1999), related to Oxisol, in the American Soil Taxonomy System (Soil Survey Staff, 1998), was studied to understand its weathering, which is poorly known in southern Brazil, and seemingly in most other subtropical environments. The Latosol is situated on plateau basalts in the southern part of Paraná Basin, which covers $\sim 1.6 \times 10^6 \text{ km}^2$ in parts of Brazil, Paraguay, Uruguay and Argentina.

Ti-magnetite and ilmenite are generally present as groundmass phases in these basalts (Picirillo *et al.*, 1988). Ti-maghemites (de Oliveira *et al.*, 1998), magnetites and maghemites (Potter and Kämpf, 1981; Gonçalves, 1987) have been described in the alteration products of these basalts. Magnetite is also present as microphenocrysts or phenocrysts in basalts, andesitic and acid rock-types (Bellieni *et al.*, 1988).

Iron oxides are important Latosol constituents. They have been considered as indicators of different pedo-environments. Schwertmann (1988) suggested that Al-goethite indicates extreme weathering soil conditions. Didier *et al.* (1985) showed that goethite and hematite result from high and low soil water activity (a_w) respectively.

The Fe-Ti minerals (Ti-magnetite, Ti-maghemite) in soil profiles from the Bushveld Complex (Fitzpatrick and Le Roux, 1975a,b), and in soils derived from mafic rocks in central and southeastern Brazil (Fabris *et al.*, 1998; Goulart *et al.*, 1998; Pinto *et al.* 1997, 1998), are unstable under tropical conditions, and undergo rapid oxidation to maghemite.

For subtropical climates as in Misiones, Argentina, Mijovilovich *et al.* (1998) reported stable magnetite in soils derived from mafic lithology. However, the subtropical zone of southern Brazil, with warm summers, mild winters and moisture all year round (Cfb of Köppen apud Strahler, 1961, p.185), has Ti-maghemite as the dominant magnetic phase in the Latosols from basalts. Thus, the origin of Ti-maghemite in subtropical climates, as in the studied area, remains unclear. Three key questions are: (1) Do the magnetic minerals of these

* E-mail address of corresponding author:
marisa.oliveira@ufrgs.br

profiles change gradually or abruptly – Ti-bearing magnetites to an Fe-oxide or hydroxide + anatase assemblage? (2) What are the changes of size, color and chemical composition of the magnetic grains? (3) Is the origin of the titanomaghemites, reported by de Oliveira *et al.* (1998), related to weathering of basalts or to pre-weathering alteration?

Here, we attempt to determine precisely the reaction sequence involving Ti-bearing minerals from the fresh basaltic rock to the upper levels of the Latosol and use petrology to support the chemical study. The evolution of magnetic minerals was defined through chemical composition, morphology and color, crystal structure and mineralogy, in the weathered profile.

METHODS

Six thin-sections from the saprock (G), the argillaceous alterite (A), the core (R) and the cortex (C) of a boulder, and the red-clay Latosol (D and F) were examined using optical microscopy, and SEM with EDS techniques. The oxides were identified under reflected light and were analyzed using an electron microprobe Cameca SX 50 (wavelength dispersive spectrometer analysis) at the Petrography Laboratory of the University of Paris VI.

After grinding rock fragments and alterites under acetone, the magnetic fractions of the samples were extracted using a hand magnet. The mineralogical analyses of samples D and F were performed by XRD using a Siemens diffractometer ($\text{CuK}\alpha$ radiation operated at 40 kV and 40 mA) at UFRGS. Samples R, C, G and A were analyzed using a Philips PW 1730 diffractometer ($\text{CoK}\alpha$ radiation, 40 kV and 40 mA) monitored by a DACO-MP computer (University of Poitiers). The scanning conditions were $0.025^\circ 2\theta$ per step and 10 s per step counting time. The peak positions were compared with those recommended by the Joint Committee on Powder Diffraction Standards (1989). Quartz was used as internal standard.

Uniform Mössbauer absorbers were prepared by separately mixing 100 mg powder of samples R and A with sugar. Sample holders were 20 mm diameter disc-shaped capsules. The spectroscopy measurements were performed in transmission geometry, using a constant-acceleration spectrometer with a $^{57}\text{Co}:\text{Rh}$ source. Calibration of velocity scale was achieved using a metallic Fe foil that was also used as the isomer shift reference.

GEOLOGICAL SETTING

The Latosol profile (Figure 1) is situated at km 287 of the road referred to as BR 116, (50°33'W, 28°05'S), in the Vacaria soil unit, classed as 'Laterítico Bruno Avermelhado' (EMBRAPA, 1988, 1999). The basalts in this area (Comin-Chiaromonti *et al.*, 1988, p. 64) are

subaphytic, composed of <0.2–0.5 mm microphenocrysts (plagioclase, augite, Ti-magnetite) in a groundmass of plagioclase, pyroxene, Ti-magnetite crystals (<0.2 mm) and glass (the ratio of crystals to glass is ~5:1). Ti-magnetite and ilmenite are present in almost all Paraná flows, mainly as groundmass and as microphenocrysts.

Weathering profiles from basaltic rocks in Paraná Basin exhibit typical lateritic zones (Table 1). The lower saprock horizon at the base of the profile contains textural and structural base relicts of the fragmented parent basaltic rock. This horizon grades upwards to the boulder facies which is associated with an argillaceous alterite, a pallid zone. The individual blocks from the boulder facies have strong yellow colors and low-density spherical cortices (halos) around the relict corestones. Bleached zones around fractures crosscut the highly porous argillaceous alterite but the original rock fabric is still conserved. A stone line consisting of boulders and fragments separates the alterite from the upper Latosol. The micromorphological terminology (matrix, plasma, glaebule, nodules) used is from the glossary of Fitzpatrick (1984).

De Oliveira *et al.* (1998) identified goethite, Al-goethite, hematite, Ti-magnetite and Ti-maghemite in the studied profile (Table 1). Goethite occurs as secondary plasma inside the altered halo of the fissure voids, which crosscut the argillaceous alterite. Al-goethite has been identified in two microsites from the boulder-altered cortex: in a very porous box-work and in secondary plasma. It was also found to be a component of the upper Latosol. Hematite occurs as mottles and nodules in the alterite and also inside the microcrystalline matrix of the Latosol.

RESULTS

The principal physical and chemical characteristics of the Fe-Ti oxides along the studied weathering profile are summarized in Table 2.

Optical microscopy (incident light)

Isotropic oxides of the saprock and the corestone of the alterite boulder are pink to brown in color with pale blue zones of higher reflectivity under reflected light. The change in color is gradual in individual grains. Cubic and incomplete skeletal forms are dominant. The opaque grains are μm size in all samples examined. Intergrowths of ilmenite of trellis type (Haggerty, 1991) appear in the {111} direction of some host crystals. Grains from the basalt cortex have more fractures than do the opaque grains of corestone. As an example, a composite grain of the alterite boulder is shown in Figure 2: a pale blue titanomaghemite from the cortex (light gray) has a titaniferous phase (dark gray) along with curved fractures. In the argillaceous alterite facies, the highly reflective isotropic oxide grains are uniformly

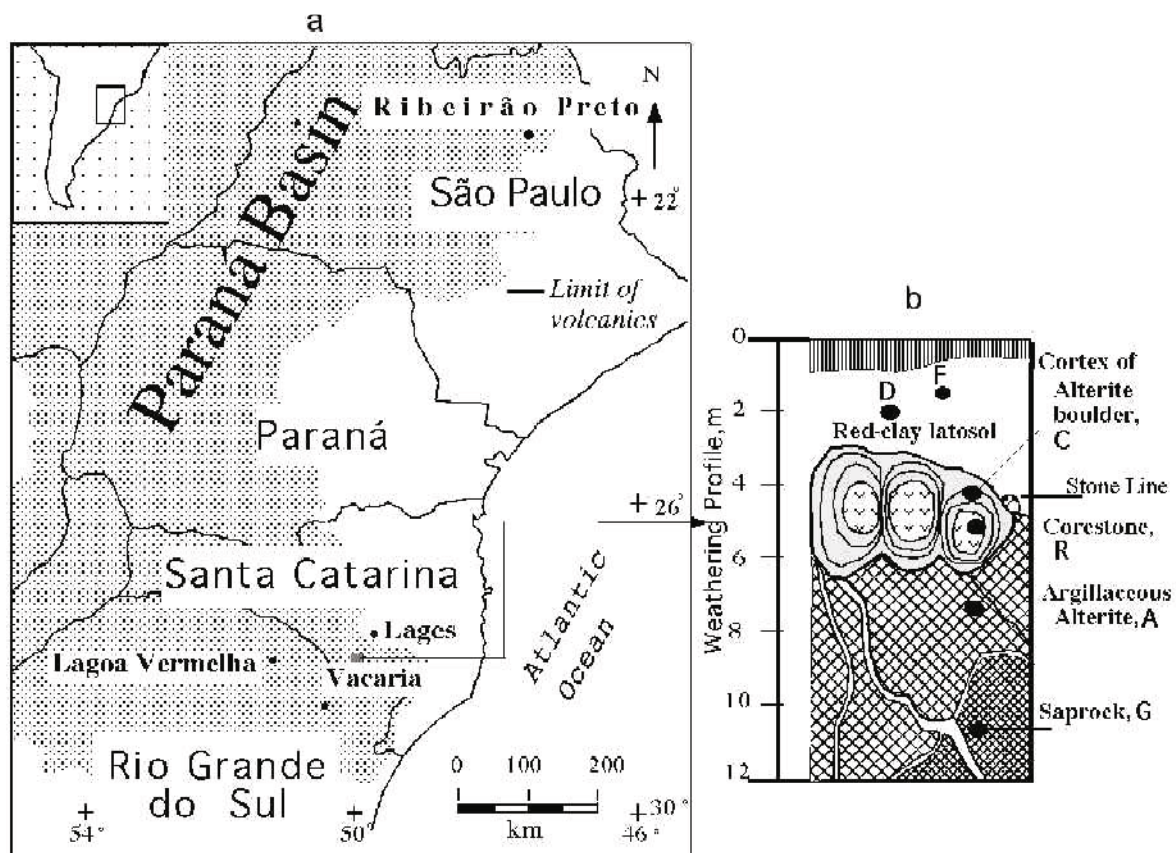


Figure 1. Location of the weathering profile over basaltic rocks in southeastern Paraná Basin (a). Position of samples in the profile (b).

pale blue in color with pinkish brown zones of oxidized magnetite (medium gray, Figure 2). All the crystals in the alterite samples have incomplete (subhedral and corroded) shapes and a large number of irregular and curved cracks. In this alterite facies, titanomaghemite grains are dispersed in a clay matrix of nontronite and kaolinite. Goethite crystals coat the fractures and cross-cut the argillaceous matrix.

The opaque grains of the Latosol are either fine grained and dispersed in the plasma or occur as glaebules as shown (Figure 2). The glaebules range in size from 0.8 to 0.2 mm, whereas the opaque grains of the matrix of the Latosol are <0.009 mm. Titanomaghemites with skeletal cubic shapes occur in the centers of glaebules. The porous microcrystalline reddish matrix inside the glaebules shows the fabric of the alterites, with pores inherited from dissolution of plagioclases. The appearance of the glaebules depends on the matrix composition: if it is opaque, the matrix contains small fragments of titanomaghemite, but if it is translucent, it does not.

Scanning electron microscopy (SEM and EDS)

Cortex. Observations, under backscattered electron mode, of a thin-section of the cortex sample (C) show

that dissolution pores are developed in titanomagnetite grains (Figure 3). Voids (black areas) exhibit negative crystal shapes. The cristobalite-K-feldspar mesostasis is partially replaced by a Si-Fe microcrystalline plasma (gray network). The Si-Fe plasma is composed of goethite, halloysite and smectite and originated from the weathering of plagioclase, clinopyroxene and micro-crystalline mesostasis. Figure 4 shows the X-ray scanning images of Fe, Ti, Mn and Al of a polymimetic oxide grain of cortex (see also Figure 2). There are different zones in the crystal: Ti-rich zones that are Fe-poor and also have some Al; Mn-rich zones; and Ti-rich zones that are also Fe-rich.

Glaebules and matrix. Titanomaghemite grains are observed inside the glaebules. These grains are fragmented as shown by the formation of dark gray Ti-rich and light gray Fe-rich zones (Figure 5a). The fragments are dissolved but the shape of the primary titanomaghemite grain is conserved in the structure of the new plasma of the glaebule (Figure 5b). The hematite glaebule exhibits an inner porous core composed of $\text{Fe} \gg \text{Al} > \text{Si} > \text{Mn} > \text{P}$ and an external lighter halo with the same composition but with a low Ti content (Figure 5c). The chemical analyses indicate that the relative propor-

Table 1. Summary description of the studied profile at km 287, federal road BR 116 (50°33'W, 28°05'S).

Profile	Field description	Microscopic and X-ray character	Interpretation
A Horizon	Dark gray-brown A horizon (10YR) is clayey textured and consists of porous aggregates up to 20 cm wide	Not studied	Present soil
Latosol matrix D	Friable, reddish brown soil horizon (5YR) with clayey texture and peds has variable thickness (2–6 m) and contains many glaebules	Soft, relict porphyritic texture has a kaolinite, goethite and hematite plasma with some grains of quartz, opaques, nodules of hematite and titanomaghemite	Reddish brown lateritic soil
Stone line	Discontinuous stone line composed of coarse fragments (up to 50 cm) of lithorelics, debris from alterites, amethyst geodes, etc., all embedded in a clayey matrix		Residual concentrate on buried slope?
Argillaceous alterite A	Argillaceous alterite with preserved rock texture, has pale red color materials (10R6/2) and patchy texture. Grayish orange pink (10R8/2) and very dusky red (10R2/2) clays fill planar pores	Halloysite pseudomorphs after plagioclase; Fe-Si-Al products after pyroxene, titanomaghemite grains, nontronites and cristobalite are interstitial. Veins filled with goethite, halloysite and manganese plasmas	Minerals transformed <i>in situ</i> (typical of pallid zones)
Cortex and corestone of alterite boulder C, R	Boulder and argillaceous alterite interspersed. Boulder alterite forms concentric dark yellowish orange (10YR6/6) shells with spongy texture around cores of unaltered basalts	Gray interiors of boulders contain microphenocrysts (Pl, Py, Ti-magnetite), a groundmass composed of (Pl, Py, Ti-magnetite) and a yellow-green birefringent mesostasis of Fe-oxide silicates that changes to isotropic dark-orange and yellow colors in the external rinds and fills all pore space. XRD of these oxide silicates shows a cryptocrystalline character. The external cortex is highly porous with 'boxworks' of Al-goethite plasma voids of dissolved phenocrysts; titanomaghemite grains fractured	Possibly a relict weathering zone?
Saprock G	Altered and fragmented country rock with yellow-orange (10YR6/6) stained boulders of fresh basalt	Microphenocrysts (Pl, Py, Ti-maghemite) are in a groundmass of (Pl, Py, Ti-magnetite). The matrix (mesostasis) presents mixed layers (smectite-glaucite) cristobalite-zeolite mixture and K-feldspars. Veins filled with halloysite	Present weathering of hydrothermally altered basalt

tions of Ti decrease from A to C while those of Fe, Si and Al increase. Some minor components (P and Mn) are concentrated during the progressive transition to hematite. The matrix of the Latosol comprises Fe, Al, Si, Ti and P.

Electron microprobe analyses

Microprobe analyses confirm that the relative proportions of TiO_2 and Fe_2O_3 of oxide grains vary in the different rock facies (Figure 6, Table 3). The concentration of TiO_2 in grains from the saprock (26.37 wt.%), argillaceous alterite (26.46 wt.%), and alterite boulder (26.88 wt.%) are all significantly greater than that of grains in the corestone (20.30 wt.%).

Minor components like Si, Al, Ca, K and Mg are thought to arise from contamination by the surrounding

silicates, namely, pyroxene debris or clay minerals such as smectite in the weakly-altered corestone and kaolinite in the altered cortex or the saprolite. It was not possible to determine if Mn is concentrated in individual small hydroxide or oxide particles or if it is included in titanomaghemite.

X-ray diffraction

The magnetic fraction of the six samples (corestone, cortex, saprock, argillaceous alterite and red-clay Latosol) has XRD patterns that correspond to those of titanomagnetites and maghemites (Figures 7, 8, 9). Titanomaghemite, which is formed by oxidation of titanomagnetite, has a defective spinel structure due to vacancies in some of the cation positions (Cornell and Schwertmann, 1996). If there is some ordering of cations

Table 2. Physical and chemical characteristics of the Fe-Ti oxides, with spinel structure, in different parts of the profile.

Profile Samples	Physical characteristics Size and shapes	Lattice parameter (Å)	Chemical characteristics Composition	$\frac{\text{Fe}+\text{Ti}}{\text{O}} \times 32^*$	$\frac{\text{Ti}}{\text{Fe}+\text{Ti}}^*$
*Latosol glaebules	Glaebules (0.5 mm) with cores, coated with secondary weathering products	8.3642 Ti-Mh	Fe > Ti >> Mg > Si	23.79	0.86
*Latosol matrix(4D)	Small grains 10–20 µm	8.3353 Mh	Fe >> Al > Si > Ti > P	20.45	0.97
Argillaceous alterite (4AmagSi)	Grains of ~90 µm; subhedral and corroded cubic crystals, with pink-brown colors and some with pale blue zones; many irregular and curved fractures	8.3440 Ti-Mh	Fe > Ti >> Al > Si > Mn	18.05	0.73
Cortex of alterite boulder (215 C)	Grains of 0.1 mm, skeletal shapes, uniform pale blue colors, more fractures, very abundant	8.3759 and 8.3457 Ti-Mh	Fe > Ti >> Al > Mn	18.19	0.71
Corestone of alterite boulder (R215mag)	Grains of 0.2 mm, cubic and skeletal shapes, pink-brown color with pale blue zones. Intergrows in the {111} direction of host crystal	8.4133 Ti-Mt	Fe > Ti >> Al > Mg > Si > Mn	18.86	0.78
Saprock (4G)	Grains of 0.2 mm, cubic and skeletal forms, pink-brown color with pale blue zones	8.3458 Ti-Mh	Fe > Ti >> Al > Si > Mn > Ca > Mg	22.14	0.68
Fresh basaltic rock (data of Bellieni <i>et al.</i> , 1988)	Groundmass phases (<0.2 mm) or microphenocrysts (0.2–0.5 mm)	Ti-Mt	Fe > Ti >> Al > Mn > Si > Mg > Cr > Ca	—	—

* Chemical ratios were calculated from EDS microanalyses

and vacancies, superstructures arise. As no superstructure reflections were observed in the diffractograms, we might conclude that these vacancies are randomly distributed in the spinel crystalline structure. Samples R (rock core, Figure 7a) and G (saprock, Figure 7c) show some other diffraction peaks (2.99 Å, 2.90 Å, 2.57 Å, 2.13 Å, 2.05 Å, 2.01 Å, 1.76 Å), probably due to lithogenic phases such as pyroxene (augite); these minerals were difficult to separate from the ferrimagnetic minerals in a sub-aphyric rock. Also, ilmenite appears in sample R although the reflections are very weak. Sample C (cortex, Figure 7b) shows two sets of maghemite diffraction peaks (Table 4). Sample A (argillaceous alterite, Figure 7d) also contains anatase. This indicates that TiO₂ is concentrated in a separate phase in sample A.

The *a* unit-cell parameter for titanomaghemite was determined from the *d*₂₂₀, *d*₄₀₀ and *d*₄₄₀ values using the equation

$$d_{hkl} = \frac{a}{\sqrt{h^2 + k^2 + l^2}}$$

(Azzároff and Buerger, 1958, p. 81).

The synthetic maghemite (γ -Fe₂O₃) diffraction peaks (JCPDS-ICDD, 1989) in the range 34–44° 2θ CoK α are indicated for comparison in Figure 8. The magnetite reflections appear only in the corestone sample (Figure 8, sample R) while maghemite replaces it in the samples of cortex (Figure 8, sample C) saprock (Figure 8, sample G) and argillaceous alterite (Figure 8, sample A). Samples D and F from the base and top of the red-clay Latosol, respectively, show reflections of kaolinite, quartz, anatase, hematite and maghemite (Figure 9, Table 6). Cristobalite (inherited from the basalt) appears in sample F (top). The reflections at 4.14 Å and 2.42 Å could be assigned to a lesser crystalline phase such as goethite. Hematite reflections are enhanced in the top of the Latosol (sample F), which may be explained as a result of the oxidation of titanomaghemite. Also, ilmenite appears in the bottom of the Latosol (sample D). The large hump in the two scans (Figure 9a,b) corresponds to fluorescence due to the Cu radiation.

Mössbauer spectra

The Mössbauer spectra of the magnetic separates are rather complicated, which is a common feature of

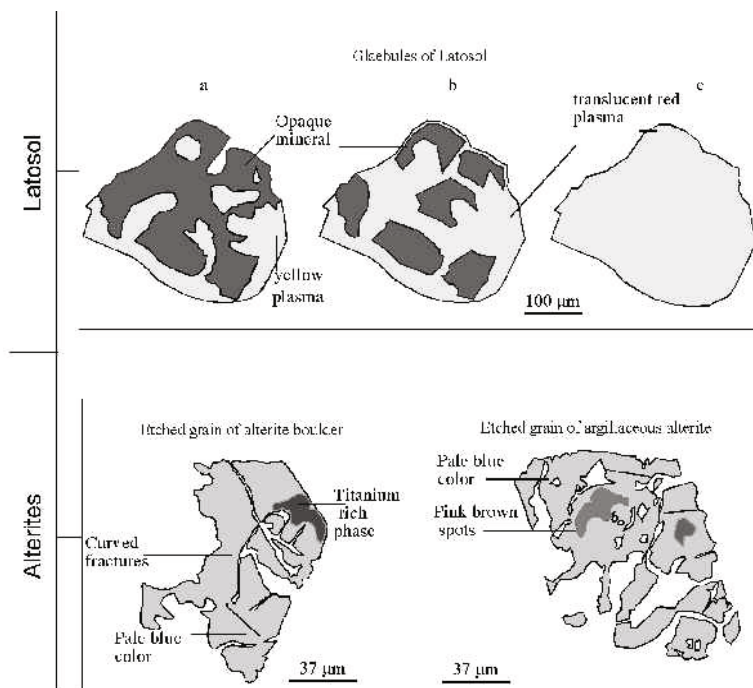


Figure 2. Optical microscopy observations of changes in single oxide grains of the alteration facies. In the upper red-clay Latosol the opaque grains are components of glaebules (a). Some glaebules show fragments dispersed in red plasma (b), other glaebules are composed of a red plasma (c). The pale blue titanomaghemite from cortex of alterite boulder shows a pink-brown titaniferous phase. Curved fractures of maghemitization cut the grain. Isotropic oxide grains in the argillaceous alterite, present uniform pale blue color and pink-brown zones of oxidized magnetite, incomplete forms and irregular, curved cracks.

magnetic soils. Chemically-disordered crystalline systems often display wide ranges of environment at the probe level, leading to effectively continuous distribution of hyperfine parameters.

In this study we have used model-independent hyperfine field distributions (HFD) to account for part of the Mössbauer spectra related to Fe magnetic species, and single sextets and doublets where the sharpness of the lines allowed us to do so (Pinto *et al.* 1998). For decomposition of the spectra we used Lorentzian line-shapes.

Transmission Mössbauer spectroscopy was used to study the magnetic separates from corestone (R) and argillaceous alterite (A), labeled R215mag and 4AmagSi, respectively.

In the R215mag separate the two characteristic magnetite sextets are relatively well defined (Figure 10). The fitted parameter values are given in Table 5. From these values, an area ratio of 1:1.61 has been calculated, which is different from the typical ratio of 1:1.88 (da Costa *et al.*, 1995a,b) for stoichiometric magnetite. Moreover, line broadening for the B-site component possibly indicates Ti replacement for Fe in octahedral sites of the magnetite structure (da Costa *et al.* 1994; Singer *et al.* 1995). There is a distinct asymmetry under the shoulder of this component as can be seen in Figure 10. We have used a HFD to account for this effect. Corresponding fitted parameters are given in Table 5. Hamdeh *et al.* (1999) reported that

for titanomagnetites, $Ti_xFe_{3-x}O_4$, in which Fe^{3+} ions are replaced by Ti^{4+} and Fe^{2+} ions, a new component appears under the shoulder of the B sextet external peaks. They report a hyperfine magnetic field of 42 Tesla and isomer shift (δ) = 0.71 mm/s at $x = 0.10$ for such a component with broad line-widths. These values are close to those reported in Table 5 for the HFD, which may thus indicate that this broadly asymmetric distribution is probably due to some Fe-Ti magnetic species in the sample. Short-range order and concentration effects can reduce the hyperfine fields and magnetic moments of Fe in magnetic systems (Krause *et al.*, 2000).

Two additional doublet components are assigned to the pyroxene augite (Bancroft, 1973), and ilmenite in very low concentration, which is in accordance with the XRD data.

Figure 11a displays the spectrum for sample A (4Amag Si) at room temperature. A doublet line structure is observed together with a sextet absorption line showing an asymmetrical line broadening. Analysis of MS results for maghemite can be difficult (Goulart *et al.*, 1998; Mussel *et al.*, 1998). We have fitted the room-temperature MS data with one doublet and one HFD whose parameters are given in Table 5. The hyperfine field at maximum probability is in accordance with those reported by Goulart *et al.* (1998) for bulk maghemite at room temperature. The doublet structure is probably related to Fe^{3+} superparamagnetic species in the sample,

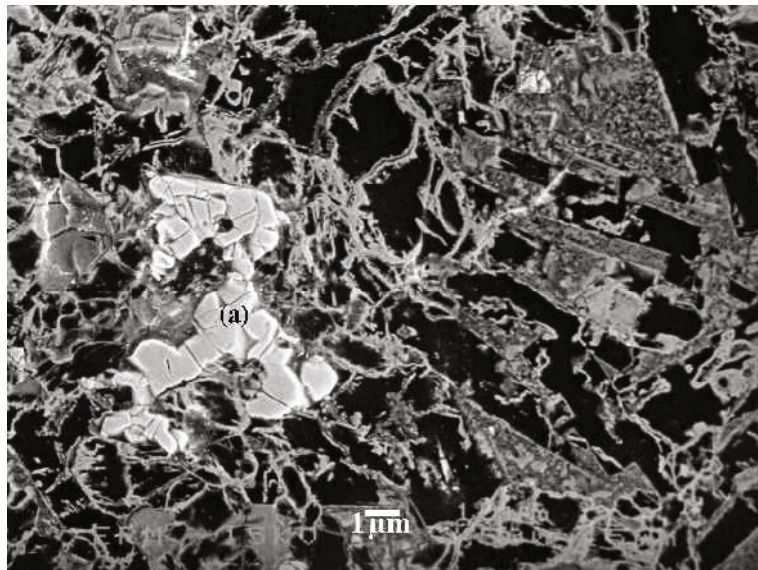


Figure 3. SEM image of titanomaghemites from the cortex of a boulder alterite. Voids correspond to black areas; the gray network corresponds to the cristobalite-K-feldspar mesostasis and Si-Fe microcrystalline plasma. This plasma is composed of goethite, halloysite and smectite. The white fragments (a) correspond to very fractured maghemite presenting dissolution features.

which seems to be corroborated by low-temperature results that are shown below.

The low-temperature spectrum (Figure 11b) shows an asymmetric sextet structure with relatively sharp lines, together with a weaker and broadened central doublet as compared to room-temperature results. According to da Costa *et al.* (1994), an acceptable model to fit low-temperature maghemite spectra is based on the assumption

that the first line (left-most absorption) of the octahedral B-site component is at higher absolute velocity than the first line of the tetrahedral A-site component. This model was used here (Figure 11b); the fitted parameters are given in Table 5. In our case, we have Ti substitution for Fe in the maghemite structure but no conclusion can be drawn with respect to the isomorphic substitution.

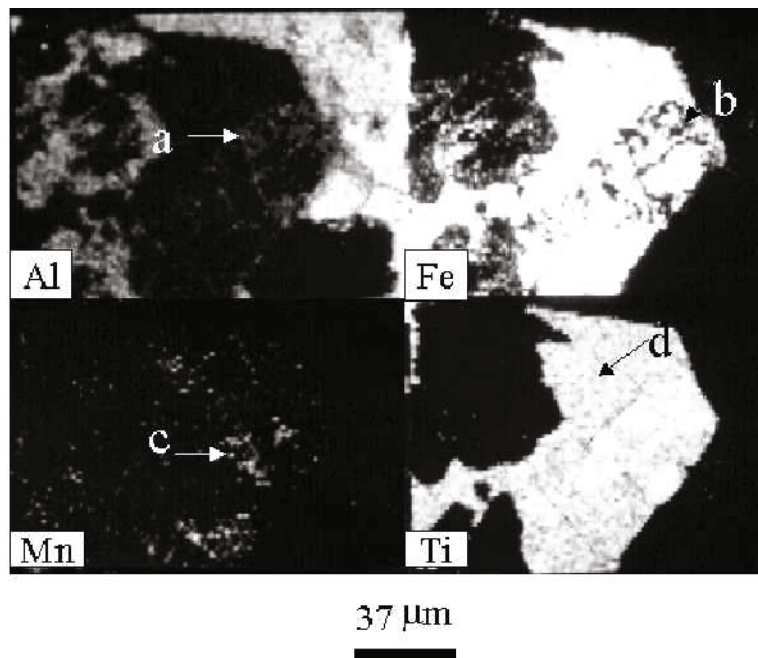


Figure 4. X-ray scanning images of Fe, Ti, Mn and Al of a polymineralic oxide grain of cortex (see Figure 2). There are different zones in the crystal: Al-rich zones (a), Ti-rich zones that are Fe poor (b) and also have some Al, Mn-rich zones (c), Ti-rich zones that are also Fe rich (d).

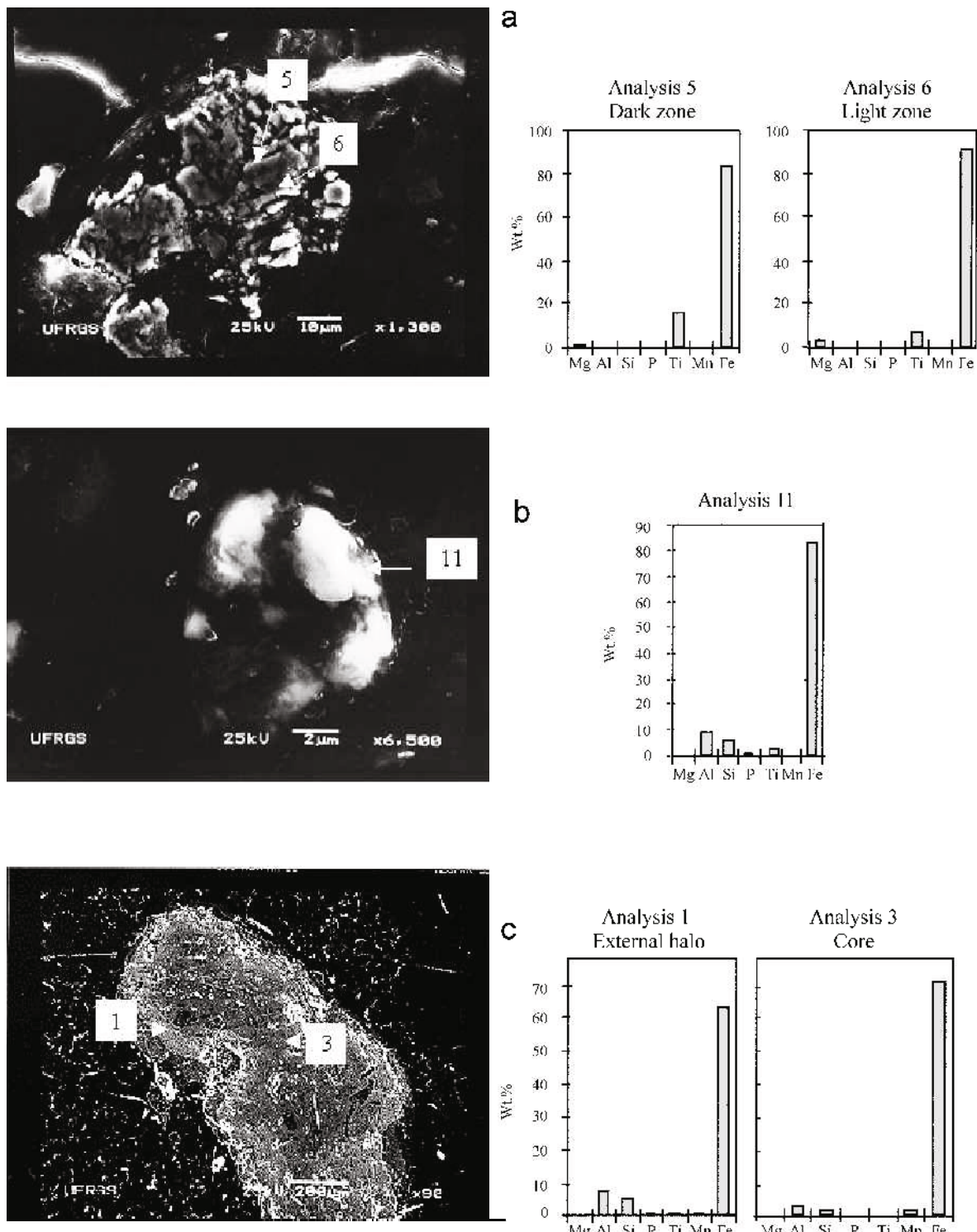


Figure 5. The thin-section of the Latosol shows titanomaghemite grains inside a glaebule of sharp borders (a). The grain is totally fragmented and shows Ti-rich zones (analysis 5) and Fe-rich zones (analysis 6). Other small grains observed in the matrix show fragments that are dissolved, but the new plasma (b) maintains the shape of the primary grain. A cartographic analysis of the components of this grain shows that it is composed of Fe > Al > Si > Ti > P. Iron concentrates in the fragments of titanomaghemite (analysis 11). The plasma around this grain is also composed of Fe, Al, Si, Ti and P. A glaebule of hematite (c) shows an inner porous matrix (analysis 3) composed of Fe >> Al > Si > Mn > P. The external halo of the glaebule has the same composition (analysis 1), with low Ti contents.

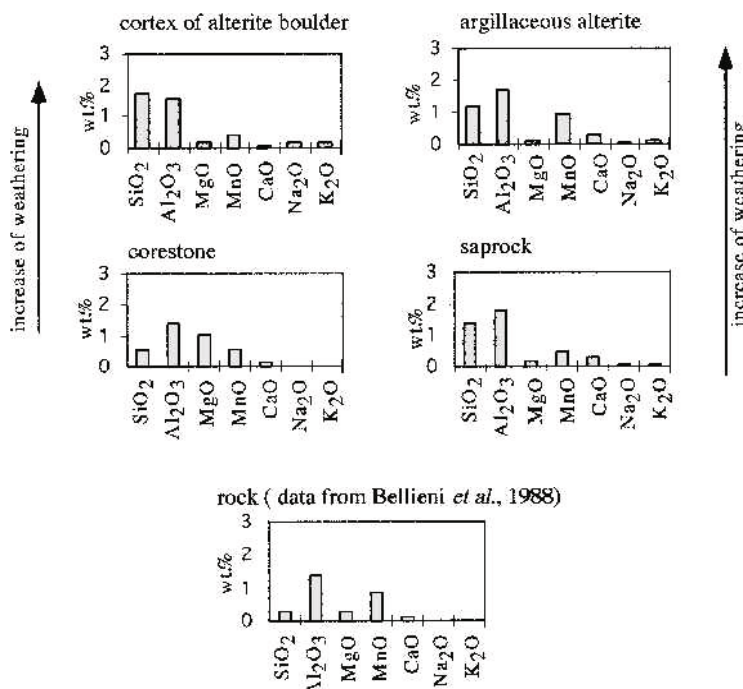


Figure 6. The impurities in Ti-maghemitic minerals of the alterite facies. Al₂O₃ and SiO₂ increase and MgO decreases from the core to the cortex of boulders. MnO increases with weathering in the argillaceous alterite.

The peaked component with broad lines in Figure 11b is the result of using a HFD to improve the data fitting at 85 K. No clear assignment can be made regarding this component, but it may be related either to Ti-Fe magnetic phases and/or superparamagnetic iron species, as suggested by the doublet line behavior whose parameters are given in Table 5.

DISCUSSION

Crystalllochemical properties of magnetic grains in the profile

Fresh basalt. Bellieni *et al.* (1986) reported titanomagnetite (unoxidized?) that crystallized at 900–1200°C, and ilmenite in almost all the Paraná flows, mainly as groundmass phases, but also as microphenocrysts. The

Table 3. Average (aver.) microprobe composition (wt.%) and standard deviation (s.d.) for titanomagnetites and titanomaghemitic minerals from samples of weathered basalts of Paraná basin, Brazil, and also atomic ratios.

Facies	Corestone (N = 13)		Cortex (N = 8)		Argillaceous alterite (N = 15)		Saprock (N = 5)	
	Titanomagnetite*		Titanomaghemite		Titanomaghemite		Titanomaghemite	
	Aver.	s.d.	Aver.	s.d.	Aver.	s.d.	Aver.	s.d.
SiO ₂	0.54	0.28	1.77	2.83	1.21	2.1	1.39	1.47
Al ₂ O ₃	1.63	0.29	1.53	0.34	1.7	0.31	1.79	0.3
Fe ₂ O ₃	72.59	1.55	65.27	7.86	66.92	5.92	63.16	4.19
MgO	1.02	0.36	0.19	0.16	0.16	0.13	0.2	0.19
TiO ₂	20.3	1.31	26.88	2.2	26.46	1.76	26.37	1.79
MnO	0.53	0.11	0.97	0.47	0.93	0.66	0.46	0.20
CaO	0.13	0.09	0.41	0.51	0.34	0.39	0.29	0.2
Na ₂ O	0.05	0.02	0.07	0.07	0.07	0.06	0.06	0.03
K ₂ O	0.05	0.02	0.33	0.33	0.17	0.23	0.06	0.06
Total	96.84	1.47	97.22	1.76	97.83	1.57	87.51	1.18
32(Fe+Ti)/O	18.86	0.17	18.19	1.31	18.06	1.41	22.14	0.68
Fe/(Fe+Ti)	0.78	0.01	0.71	0.04	0.73	0.08	0.68	0.03

N = Number of analyses

*Titanomagnetites have Fe³⁺ as well as Fe²⁺ in the structure, but we could not evaluate their ratios

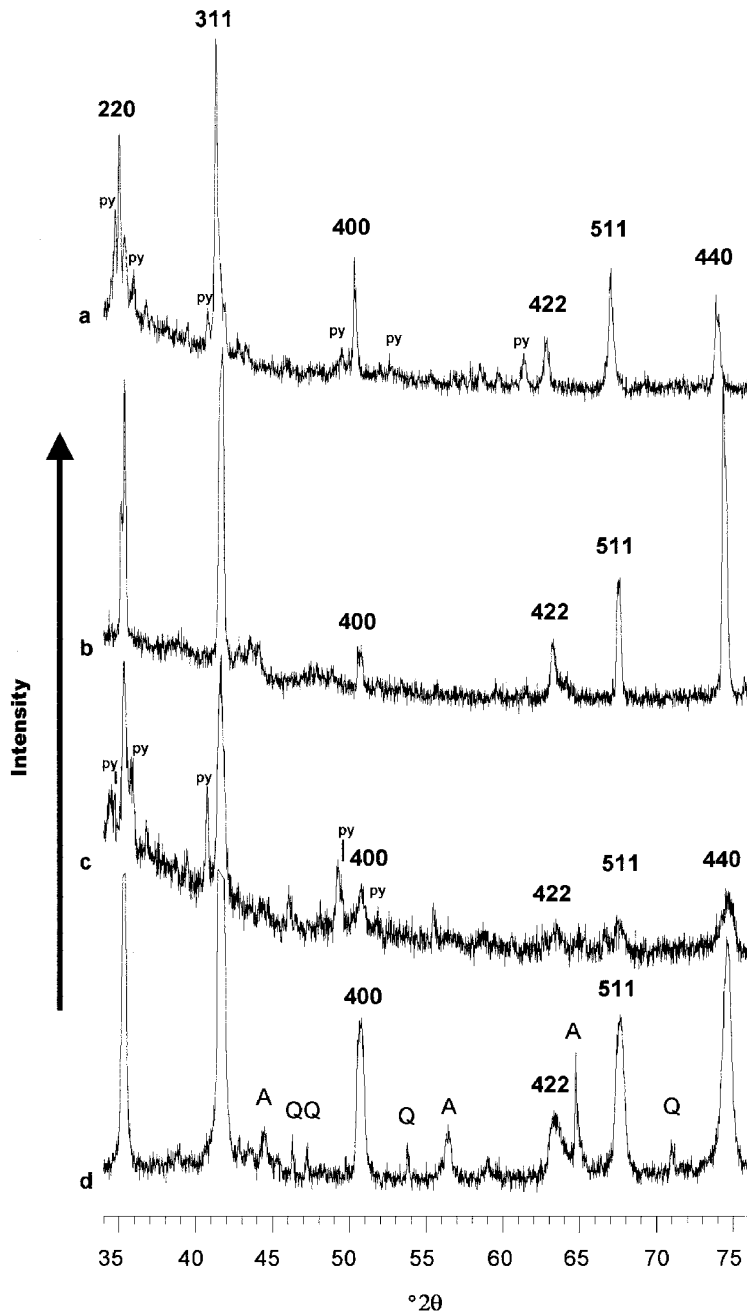


Figure 7. XRD patterns with principal reflections of the magnetic fraction of (a) corestone and (b) cortex of boulder alterite; from (c) saprock and (d) from argillaceous alterite. The following minerals were also identified: A (anatase) and also Q (quartz) that was added as a standard. Other reflections are related to lithogenic phases as pyroxene-augite (py).

average composition of titanomagnetites (35 microprobe analyses) from the low-Ti basalts from southern Paraná flows is TiO_2 (24.71%), FeO_t (69.90%), Al_2O_3 (1.36%), MnO (0.86%), SiO_2 (0.28%), MgO (0.26%), Cr_2O_3 (0.12%) and CaO (0.12%). The main mineralogical phases of these Brazilian geomaterials are 70.44% ulvöspinel solid-solutions (Bellieni *et al.*, 1988). The average representative compositions for Ti-magnetites

from basalts and intermediate rock types from Paraná flows are not significantly different.

Saprock. The 0.2 mm wide grains exhibit cubic and skeletal shape and are pinkish brown colored with pale blue zones. The calculated unit-cell parameter, a , in the saprock is 8.3458 Å which corresponds to values for titanomaghemite: 8.3475 Å (Basta, 1959), 8.341 Å

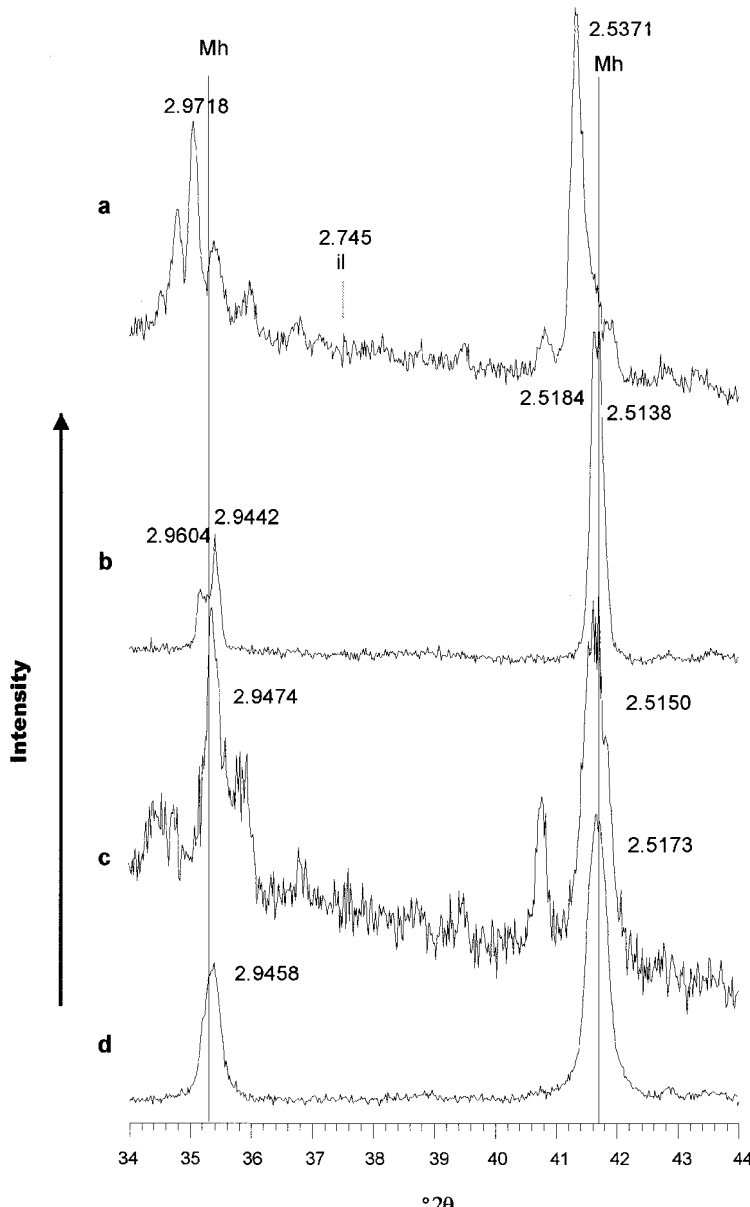


Figure 8. XRD patterns between 34 and 44°2θ (CoK α), of the same samples as in Figure 7. Corestone (a) presents magnetite reflections; cortex (b), saprock (c) and argillaceous alterite (d) present maghemite reflections. Lines marked Mh correspond to the positions of standard maghemite-C, syn (JCPDS-ICDD, 1989).

(Collyer *et al.*, 1988), 8.348 Å (Allan *et al.*, 1989). The principal impurities are Al, Si, Mn, Ca and Mg. The atomic proportion of metals relative to oxygen, [(Fe+Ti)/O] \times 32, is 22.14. It is less than that calculated by Akimoto and Katzura (1959) for titanomagnetites from volcanic rocks of Japan: 24.80–22.40. This implies that the Fe content of the titanomaghemites studied here is less than that of Japan.

Corestone. The 0.2 mm wide grains with cubic and skeletal shapes are pinkish brown colored with pale blue zones. The *a* unit-cell parameter of the magnetic

separate, is the largest of all the altered facies: at 8.4133 Å and corresponds to a titanomagnetite. The principal impurities of the grains are Al and Mg which possibly replace Fe³⁺ and Fe²⁺, respectively, in the titanomagnetite octahedral sites (Sanver and O'Reilly, 1970). Manganese is also one of the principal impurities of titanomagnetite in basalts (Bellieni *et al.*, 1988).

The atomic proportion of metals to oxygen, [(Fe+Ti)/O] \times 32, is 18.86 and is less than in saprock grains, which implies a loss of Fe ions. The Mössbauer spectra of the sample R (R215mag) confirm that these grains are oxidized titanomagnetite (non-stoichiometric). In spite

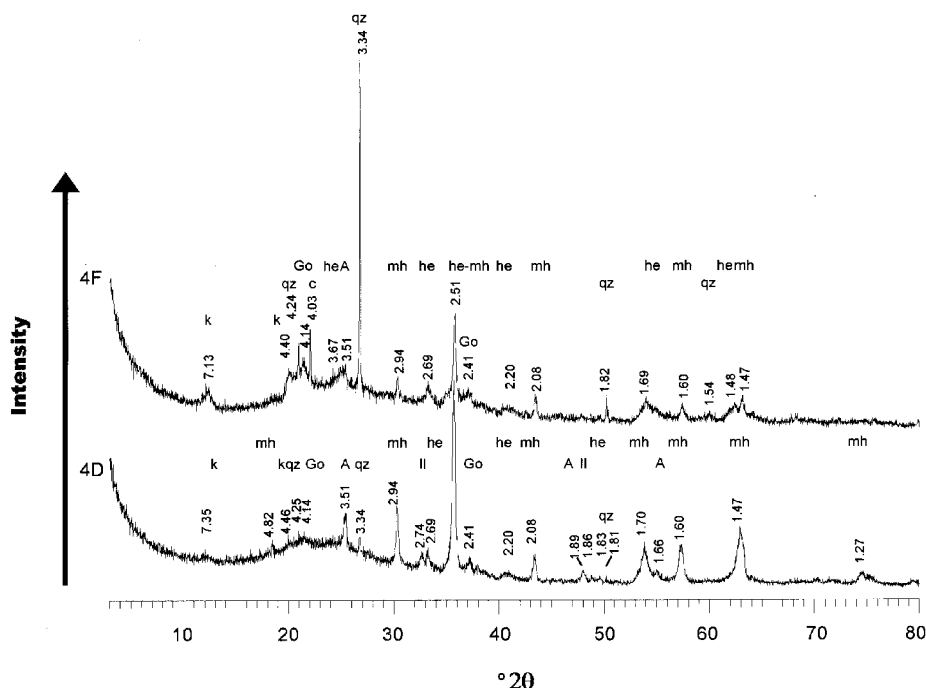


Figure 9. XRD patterns of the lower and upper Latosol (spacings in Å). The principal constituents are kaolinite (k), quartz (qz), anatase (A), hematite (he), maghemite (mh) and cristobalite (c). Goethite (Go) is poorly identified. Hematite reflections are enhanced in the upper part of the Latosol, which may be explained as a result of oxidation of titanomaghemite. Also, ilmenite (II) appears in the bottom of the Latosol.

of the fact that oxidized titanomagnetite may be generated under certain magmatic conditions (Sanver and O'Reilly, 1970), it seems likely that, here, they are an early stage of weathering.

Argillaceous alterite. Grains (90 µm wide) are subhedral corroded cubic crystals with pinkish brown colors (some crystals show pale blue zones) and many irregular and curved fractures. The a unit-cell parameter value (8.3440 Å) is the smallest of all the facies. The principal impurities of the grains are Al that might replace Fe³⁺ and Mn. The atomic proportion of metals to oxygen, 18.05, is lower than that of saprock and corestone grains

showing that the Fe ion loss increases with weathering intensity. The Mössbauer data agree very well with those of the synthetic Al-substituted maghemites reported by da Costa *et al.* (1994).

Cortex of boulder alterite. Magnetic grains (0.1 mm wide) exhibit corroded skeletal shapes, uniform pale blue colors and many fractures. The two sets of maghemite diffraction peaks (Table 4) may be related to different weathering conditions in the concentric alteration halos of this facies. One of the calculated values for the a unit-cell parameter (8.3457 Å) is lower than that from grains in the rock core and corresponds to

Table 4. The d -values of reflections from magnetic minerals from the profile, from titanomaghemites (Basta, 1959), from maghemite-C (syn.) and the a parameter* (all values in Å).

	220	311	400	422	511	440	a
R215mag	2.9718	2.5371	2.1031	1.7141	1.6201	1.4888	8.4133*
215C	2.9604	2.5184	2.0953	1.7073	1.6104	1.4802	8.3759*
215C	2.9442	2.5138	2.0861	1.7054	1.6074	1.4788	8.3457*
4G	2.9474	2.5150	2.0853	1.7006	1.6125	1.4778	8.3458*
4AmagSi	2.9458	2.5173	2.0861	1.7049	1.6057	1.4771	8.3440*
Ti maghemite (Basta, 1959)	2.949	2.515	2.084	1.703	1.605	1.474	8.3475
Maghemite-C	2.953	2.5177	2.0886	1.7015	1.6073	1.4758	8.3515

* calculated from the d_{220} , d_{400} and d_{440} values using the equation:

$$d_{hkl} = \frac{a}{\sqrt{h^2 + k^2 + l^2}}$$

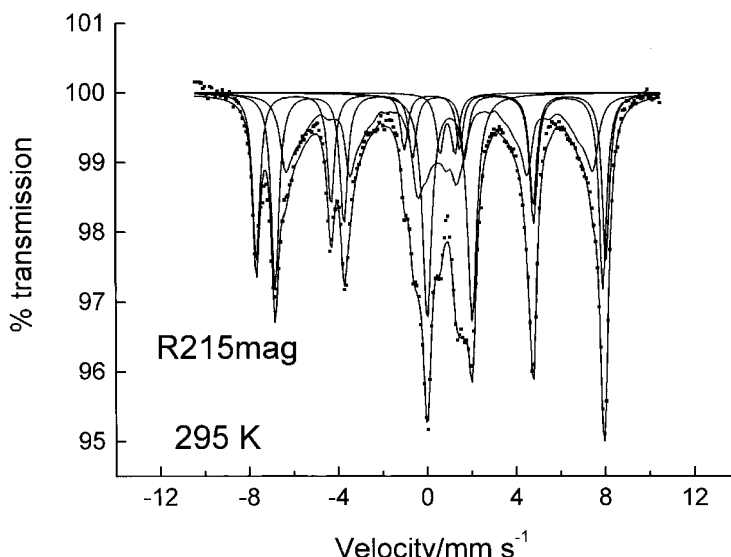


Figure 10. Mössbauer spectra from sample R215mag at 295 K. The two characteristic magnetite sextet lines with a superposition at the positive high velocity are strongly marked.

values of synthetic maghemite (Table 4). The other calculated a parameter value (8.3759 Å) is intermediate between titanomaghemite and titanomagnetite. In addition, Mn impurities are significantly higher than in the other facies. Frost and Lindsley (1991) explained this variability in oxides as a reflection of the speed at which spinels tend to undergo cation exchange with other minerals.

Upper soils. Small Ti-maghemite grains (~8 µm wide) exhibit the smallest a unit-cell parameter value (8.3353 Å). They are Ti depleted compared to Ti-maghemite grains from the underlying alterites. Some Ti ions contribute to the formation of anatase. At the same time, the reddish and translucent glaebules (0.8–0.2 mm in size), with no fragments of titanomaghemites from the alterite, are transformed into hematite glaebules, of which the external zones are slightly enriched in Ti. This 'titanohematite' may possibly be a

titanomaghemite weathering end-product in the Latosol (Fitzpatrick and LeRoux, 1975b).

The titanomagnetite to titanomaghemite conversion process

In the subtropical zone of southern Brazil, the titanomagnetite crystals from the fresh Paraná basalt are progressively altered to a hematite + anatase assemblage through an intermediate mineral phase: the titanomaghemite (Table 6). The chemical composition of this phase changes gradually from the less-altered facies (corestone) to the other facies. The Fe/(Fe+Ti) ratio decreases from 0.78 (corestone), 0.73 (argillaceous alterite), 0.71 (cortex) to 0.68 (saprock). This could indicate that titanomagnetite is a solid-solution phase whose composition is controlled by local chemical conditions. The oxidation begins with addition of oxygen and internal diffusion of Fe²⁺ towards the exterior of the crystals, which eventually grow a little. The amounts of TiO₂ increase from the spinels of the rock

Table 5. Mössbauer parameters for samples at selected temperatures.

Magnetic Extracts	T (K)	Hhf (Tesla)	2ε _Q (mm/s)	δ (mm/s)	Γ (mm/s)	RA %	ΔE _Q (mm/s)	δ (mm/s)	Γ (mm/s)	RA%	
R215mag	295K	49	—	0.29	0.40	18	mg (A)	1.99	1.12	0.57	19
		46	—	0.63	0.52	29	mg (B)	0.70	1.04	0.30	2
		43(*)	-0.10	0.54	0.66(**)	32	(Fe,Ti) species				aug (pyr)
4AmagSi	295K	50(*)	—	0.28	0.57	95	mh	0.48	0.33	0.35	5
		53	—	0.46	0.45	34	mh (B)	0.54	0.41	0.69	5
		51	—	0.38	0.47	34	mh(A)				Fe ³⁺ sp
		46(*)	—	0.68	0.60(**)	27	Fe ³⁺				Fe ³⁺ sp

RA: relative area; mg: magnetite; mh: maghemite; aug (pyr): augite (pyroxene); ilm: ilmenite; A: tetrahedral site; B: octahedral site; 2ε_Q: quadrupole splitting; ΔE_Q quadrupole splitting for (super) paramagnetic Fe; sp: superparamagnetic; (*) hyperfine field at maximum probability; (**) line-width for individual component of the hyperfine field distribution.

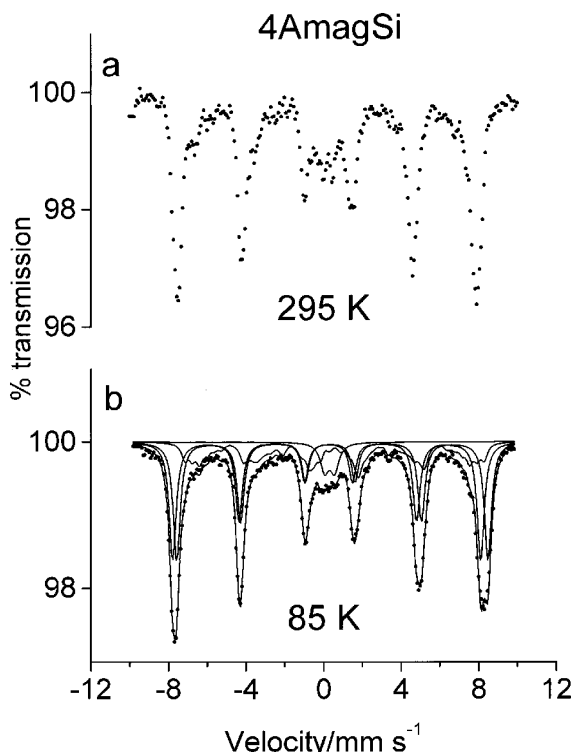


Figure 11. Mössbauer spectra from sample 4AMAG Si at 295 K and at 85 K. (a) Mössbauer spectrum for sample 4AMAG Si at room temperature. A double line structure is apparent from the data together with sextet absorption lines with asymmetrical line broadening. (b) Lowering of sample temperature to 85 K. It shows a six asymmetric line structure where the central doublet is almost gone.

core to the grains in the alterites. The a unit-cell parameter value decreases with increasing oxidation. However, a clear relationship between the amounts of Ti and a parameter was not found. At the top of the profile,

over the stone line, there are different pedoenviroment conditions and the alterite texture is destroyed. Titanium is released by oxidation of titanomaghemit and is dispersed as small anatase grains in the Latosol. Titanomaghemites of the Latosol have minimal Ti contents during the transformation into hematite + anatase.

The alteration process described may be ancient, related not only to the present mild conditions but also to tropical paleoclimates that prevailed in the study area.

CONCLUSIONS

Non-stoichiometric titanomagnetite of the original basalt in the rock cores of the weathering profiles is unstable and alters towards the surrounding alterites, into a metastable phase, titanomaghemit. This Fe-Ti oxide with spinel structure has more fractures, mottled colors, increased and changed impurities, lower atomic proportions of metals to oxygen, and a lower a parameter when compared to titanomagnetite.

The alteration is a gradual process. Its intensity is less in the rock cores, and medium to high from the internal to external alteration cortex where oxidized titanomaghemit was found to occur. As the preserved rock texture of the alterites is destroyed, red-clay Latosol forms at the top of the weathering profiles and titanomaghemit is destabilized. It transforms into a hematite + anatase assemblage in the matrix of the red-clay Latosol or it is preserved in some soil glaebules inherited from the alterites. From this observed evolutionary trend we may conclude that the Fe-Ti oxides of these weathering profiles are indicators of different pedo-environments.

Sub-tropical climatic conditions are not reported in the literature to be associated with the instability in titanomagnetite. Nevertheless, the local climate of the

Table 6. Alteration of titanomagnetite in weathering profiles developed on Paraná basalts, southern Brazil.

Profile		Chemistry	Morphology and color	Structure	Mineralogy	Intensity of weathering
Above the Stone line	Matrix	Low metal/oxygen ratios; many kinds of impurities; low Ti	Very small grains; uniform color	Smallest a parameter 8.3353 Å	Maghemite with very low Ti content; hematite with Ti	Highest
	Glaebules	High metal/oxygen ratios; two types of impurities Mn, Al; high Ti content	Intensely fractured grains; spotted color	Intermediate a parameter 8.3642 Å	Titanomaghemit	Medium to high
Below the Stone line	Alterites	Low metal/oxygen ratios; Mn, Al impurities; high Ti	Increase of fractures; mottled colors	a parameter from 8.3759 to 8.3440 Å	Titanomaghemit	Medium to high
	Rock cores	High metal/oxygen ratios; more diverse impurities, and Ti	Few fractures; mottled colors	Highest a parameter 8.4133 Å	Titanomagnetite	Minimal to absent

studied area, with year-round moisture as well as a long history of tropical paleoclimates may be responsible for the successive periods of oxidation that resulted in the evolutionary trend: titanomagnetite–titanomaghemite–hematite.

ACKNOWLEDGMENTS

This work was supported financially by CAPES/COFECUB 108/90 and 185/96, CNPQ process 400043/96-3, PRONEX 76.97.1006.00 and PROPESQ/UFRGS. The authors thank Dr G. Stoops, Dr J.D. Fabris and Dr H. Stanjek for their careful reviews, Dr P.E. Potter for his careful revision and Dr N. Dani (UFRGS) for help with the illustrations.

REFERENCES

- Akimoto, S. and Katzura, T. (1959) Magneto-chemical study of the generalized titanomagnetite in volcanic rocks. *Journal of Geomagnetism and Geoelectricity*, **3**, 69–90.
- Allan, J.E.M., Coey, J.M.D., Sanders, I.S., Schwertmann, U., Friedrich, G. and Wiechowski, A. (1989) An occurrence of fully-oxidized natural titanomaghemite in basalt. *Mineralogical Magazine*, **53**, 299–304.
- Azzároff, L.V. and Buerger, M.J. (1958) *The Powder Method in X-ray Crystallography*. McGraw-Hill Book Company, New York, 342 pp.
- Bancroft, G.M. (1973) *Mössbauer Spectroscopy – an Introduction for Inorganic Chemists and Geochemists*. McGraw-Hill Book Company (UK) Limited, p. 168–177.
- Basta, E.Z. (1959) Some mineralogical relationship in the system Fe_2O_3 – Fe_3O_4 and the composition of titanomaghemite. *Economic Geology*, **54**, 698–719.
- Bellieni, G., Comin-Chiaromonti, P., Marques, L.S., Martinez, L., Melfi, A.J., Pacca, I.G. and Piccirillo, E. (1986) Petrogenetic aspects of acid and basaltic lavas from Paraná plateau (Brazil): geological, mineralogical and petrochemical relationships. *Journal of Petrology*, **27**, 915–944.
- Bellieni, E.M., Comin-Chiaromonti, P., Bellieni, G., Civetta, L., Marques, L.S., Melfi, A.J., Petrini, R., Raposo, M.I.B. and Stolfa, D. (1988) Petrogenetic aspects of continental flood basalt–rhyolite suites from the Paraná Basin (Brazil). Pp. 179–205 in: *The Mesozoic Flood Volcanism of the Paraná Basin, Petrogenetic and Geophysical Aspects* (E.M. Piccirillo, and A.J. Melfi, editors). Instituto Astronômico e Geofísico, São Paulo, Brazil.
- Camargo, M.N., Klamt, E. and Kauffman, J.H.B. (1987) Classificação de solos usada em levantamentos pedológicos no Brasil. *Boletim Informativo Sociedade Brasileira de Ciência do Solo. Campinas*, **12**, 11–33.
- Collyer, S., Grimes, N.W., Vaughan, D.J. and Longworth, G. (1988) Studies of the crystal structure and crystal chemistry of titanomaghemite. *American Mineralogist*, **73**, 153–160.
- Comin-Chiaromonti P., Bellieni, G., Piccirillo E.M. and Melfi, A.J. (1988) Classification and petrography of continental stratoid volcanics and related intrusives from the Paraná Basin (Brazil) Pp. 47–78 in: *The Mesozoic Flood Volcanism of the Paraná Basin, Petrogenetic and Geophysical Aspects* (E.M. Piccirillo, and A.J. Melfi, editors). Instituto Astronômico e Geofísico, São Paulo, Brazil.
- Cornell, R.M. and Schwertmann, U. (1996) *The Iron Oxides. Structures, Properties, Reactions, Occurrence and Uses*. VCH, Weinheim, Germany, 573 pp.
- da Costa, G.M., de Grave, E., Bowen, L.H. and Vandenberghe, R.E. (1994) The center shift in Mössbauer spectra of maghemite and aluminum maghemites. *Clays and Clay Minerals*, **42**, 628–633.
- da Costa, G.M., de Grave, E., Bowen, L.H., De Bakker, P.M.A. and Vandenberghe, R.E. (1995a) Variable-temperature Mössbauer spectroscopy of nanosized maghemite and Al-substituted maghemites. *Clays and Clay Minerals*, **43**, 562–568.
- da Costa, G.M., de Grave, E., De Bakker, P.M.A. and Vandenberghe, R.E. (1995b) Influence of non stoichiometry and the presence of maghemite on the Mössbauer spectrum of magnetite. *Clays and Clay Minerals*, **43**, 656–668.
- de Oliveira, M.T.G., Formoso, M.L.L., Trescases, J.J. and Meunier, A. (1998) Clay mineral facies and lateritization in basalts of the southeastern Paraná Basin, Brazil. *Journal of South American Earth Sciences*, **11**, 365–377.
- Didier, P., Perret, D., Tardy, Y. and Nahon, D. (1985) Equilibres entre kaolinites ferrifères, goethites alumineuses et hématites alumineuses dans les systèmes cuirassés. Rôle de l'activité de l'eau et de la taille des pores. *Science Géologique Bulletin*, **38**, 383–397.
- EMBRAPA (Empresa Brasileira de Pesquisa Agropecuária) (1988) Serviço nacional de Levantamento e Conservação de Solos (Rio de Janeiro, RJ). *Sistema Brasileiro de Classificação de Solos: 3. Aproximação*. Rio de Janeiro, Brazil, 122 pp. (Mimeografado).
- EMBRAPA (Empresa Brasileira de Pesquisa Agropecuária) (1999) Centro Nacional de Pesquisa de Solos (Rio de Janeiro, RJ). *Sistema Brasileiro de Classificação de Solos, Brasília*. Embrapa Produção de Informação, Rio de Janeiro, Brazil, 412 pp.
- Fabris, J.D., Coey, J.M.D. and Mussel, W. da N. (1998) Magnetic soils from mafic lithodomains in Brazil. *Hyperfine Interactions*, **113**, 249–258.
- Fitzpatrick, E.A. (1984) *Micromorphology of Soils*. Chapman & Hall, New York, 433 pp.
- Fitzpatrick, R.W. and Le Roux, J. (1975a) Mineralo-chemical studies on titaniferous red soils of varying base status and structure. Pp. 344–375 in: *Proceedings of the 6th Congress of the Soil Science Society of South Africa (Blyde River)* (M.E. Sumner, editor). Soil Science Society of South Africa, Pretoria.
- Fitzpatrick, R.W. and Le Roux, J. (1975b) Pedogenic and solid solution studies on iron titanium oxides. Pp. 585–599 in: *Proceedings of the International Clay Conference, Mexico City, 1975* (S.W. Bailey, editor). Applied Publishing, Willmette, Illinois.
- Frost, B.R. and Lindsley, D.H. (1991) Occurrence of iron titanium oxides in igneous rocks. Pp. 433–462 in: *Oxide Minerals: Petrologic and Magnetic Significance* (D.H. Lindsley, editor). Reviews in Mineralogy **25**, Mineralogical Society of America, Washington, D.C.
- Gonçalves, N.M.M. (1987) Transformações Mineralógicas e Estruturais relacionadas à Alteração Hidrotermal e Intempérica de Rochas Vulcânicas Básicas da Bacia do Paraná Setentrional – Região de Ribeirão Preto – S.P. Brazil. Tese de Doutoramento, Universidade de São Paulo, Brazil, 212 pp.
- Goulart, A.T., Fabris, J.D., Jesus Filho, M.F., Coey, J.M.D., da Costa, J.M. and de Grave, E. (1998) Iron oxides in a soil developed from basalt. *Clays and Clay Minerals*, **46**, 369–378.
- Haggerty, S.E. (1991) Oxide textures – a mini atlas. Pp. 129–137 in: *Oxide Minerals: Petrologic and Magnetic Significance* (D.H. Lindsley, editor). Reviews in Mineralogy **25**, Mineralogical Society of America, Washington, D.C.
- Hamdeh, H.H., Barghout, K., Ho, J.C., Shand, P.M. and Miller, L.L. (1999) A Mössbauer evaluation of cation distribution in titanomagnetites. *Journal of Magnetism and Magnetic Materials*, **191**, 72–78.
- Joint Committee on Powder Diffraction - International Center

- for Diffraction Data Standards, Copyright (1989), Powder Diffraction Files -2, PDF 39-1346.
- Krause, J.C., Schaf, J., da Costa Jr., M.I. and Paduani, C. (2000) Effects of composition and short-range order on the magnetic moments of Fe in $\text{Fe}_{1-x}\text{V}_x$ alloys. *Physical Review B*, **61**, 6196–6204.
- Mijovilovich, A., Morras, H., Saragovi, C., Santana, G.P. and Fabris, J.D. (1998) Magnetic fraction of an Ultisol from Misiones, Argentina. *Hyperfine Interactions C*, **3**, 332–335.
- Mussel, W. da N., Fabris, J.D. and Coey, J.M.D. (1998) Titanomaghemites obtained by oxidation of natural titanomagnetites. *Hyperfine Interactions C*, **3**, 358–351.
- Picirillo, E.M., Comin Chiaromonti, P., Melfi, A.J., Stolfa, D., Bellieni, G., Marques, L.S., Giarettta, A., Nardy, A.J.R., Pinse, J.P.P., Raposo, M.I.B. and Roisenberg, A. (1988) Petrochemistry of continental flood basalt-rhyolite suites and related intrusives from the Paraná Basin (Brazil). Pp. 107–156 in: *The Mesozoic Flood Volcanism of the Paraná Basin, Petrogenetic and Geophysical Aspects* (E.M. Picirillo and A.J. Melfi, editors). Instituto Astronômico e Geofísico, São Paulo, Brazil.
- Pinto, M.C.F., Fabris, J.D., de Jesus Filho, M.F., Coey, J.M.D., Mussel, W. da N. and Goulart, A.T. (1997) Iron-rich spinels from Brazilian soils. *Hyperfine Interactions*, **110**, 23–32.
- Pinto, M.C.F., Fabris, J.D., Goulart, A.T. and Santana, G.P. (1998) Pedogenetic instability of magnetite in mafic lithology. *Hyperfine Interactions C*, **3**, 325–327.
- Potter, R.O. and Kämpf, N. (1981) Argilo-minerais e óxidos de ferro em cambissolos e latossolos sob regime climático térmico údico no Rio Grande do Sul. *Revista Brasileira de Ciência do Solo*, **5**, 153–159.
- Readman, P.W. and O'Reilly, W. (1970) The synthesis and inversion of non-stoichiometric titanomagnetites. *Physics of the Earth and Planetary Interiors*, **4**, 121–128.
- Resende, M., Curi, N., Resende, S.B. de and Corrêa, G.F. (1995) *Pedologia: Base para Distinção de Ambientes*. NEPUT, Viçosa (MG, Brazil), 304 pp. (in Portuguese).
- Sanver, M. and O'Reilly, W. (1970) The identification of naturally occurring non-stoichiometric titanomagnetites. *Physics of the Earth and Planetary Interiors*, **2**, 166–174.
- Schwertmann, U. (1988) Occurrence and formation of iron oxides in various pedoenvironments. Pp. 267–302 in: *Iron in Soils and Clay Minerals* (J.W. Stucki, B.A. Goodman and U. Schwertmann, editors). NATO ASI series, **C217**, D. Reidel Publishing Company, Dordrecht, The Netherlands.
- Singer, M.J., Bowen, L.H., Verosub, K.L., Fine, P. and Tenpas, J. (1995) Mössbauer spectroscopic evidence for citrate-bicarbonate-dithionite extraction of maghemite from soils. *Clays and Clay Minerals*, **43**, 1–7.
- Soil Survey Staff, SCS, USDA (1998) *Keys to Soil Taxonomy*, 8th edition. USDA, Washington, D.C.
- Strahler, A. (1961) *Physical Geography, second edition*. John Wiley & Sons Inc., New York, 534 pp.

(Received 15 March 2000; revised 3 January 2002; Ms. 435; A.E. Helge Stanjek)